

Article

Characterizing Optimum N Rate in Waterlogged Maize (*Zea mays* L.) with Unmanned Aerial Vehicle (UAV) Remote Sensing

Bhawana Acharya ¹, Syam Dodla ², Brenda Tubana ³, Thanos Gentimis ⁴, Fagner Rontani ⁵, Rejina Adhikari ⁶, Dulis Duron ³, Giulia Bortolon ³ and Tri Setiyono ^{3,*}

¹ Department of Environmental Sciences, University of California, Riverside, CA 92521, USA; bhawana.acharya@email.ucr.edu

² International Fertilizer Development Center, Muscle Shoals, AL 35661, USA; sdodla@ifdc.org

³ School of Plant, Environmental and Soil Sciences, Louisiana State University, Baton Rouge, LA 70803, USA

⁴ Department of Experimental Statistics, Louisiana State University, Baton Rouge, LA 70803, USA; tgentimis@agcenter.lsu.edu

⁵ Natural Resource Sciences, North Dakota State University, Fargo, ND 58102, USA

⁶ Global Geospatial Institute, 8000 Innovation Park Drive, Baton Rouge, LA 70820, USA

* Correspondence: tsetiyono@agcenter.lsu.edu; Tel.: +1-225-578-3135

Abstract: High soil moisture due to frequent excessive precipitation can lead to reductions in maize grain yields and increased nitrogen (N) loss. The traditional methods of computing N status in crops are destructive and time-consuming, especially in waterlogged fields. Therefore, in this study, we used unmanned aerial vehicle (UAV) remote sensing to evaluate the status of maize under different N rates and excessive soil moisture conditions. The experiment was performed using a split plot design with four replications, with soil moisture conditions as main plots and different N rates as sub-plots. The artificial intelligence SciPy (version 1.5.2) optimization algorithm and spherical function were used to estimate the economically optimum N rate under the different treatments. The computed EONR for CRS 2022 was 157 kg N ha^{-1} for both treatments, with the maximum net return to N of USD 1203 ha^{-1} . In 2023, the analysis suggested a lower maximum attainable yield in excessive water conditions, with EONR pushed up to 197 kg N ha^{-1} as compared to 185 kg N ha^{-1} in the control treatment, resulting in a lower maximum net return to N of USD 884 ha^{-1} as compared to USD 1019 ha^{-1} in the control treatment. This study reveals a slight reduction of the fraction of NDRE at EONR to maximum NDRE under excessive water conditions, highlighting the need for addressing such abiotic stress circumstances when arriving at an N rate recommendation based on an N-rich strip concept. This study confirms the importance of sensing technology for N monitoring in maize, particularly in supporting decision making in nutrient management under adverse weather conditions.

Keywords: maize; N fertilizer; yield; unmanned aerial vehicle (UAV); normalized difference red edge index (NDRE); normalized difference vegetation index (NDVI); economically optimum N rate (EONR); spherical function; artificial intelligence; SciPy



Academic Editors: Biquan Zhao and Cengiz Koparan

Received: 25 December 2024

Revised: 6 February 2025

Accepted: 8 February 2025

Published: 10 February 2025

Citation: Acharya, B.; Dodla, S.; Tubana, B.; Gentimis, T.; Rontani, F.; Adhikari, R.; Duron, D.; Bortolon, G.; Setiyono, T. Characterizing Optimum N Rate in Waterlogged Maize (*Zea mays* L.) with Unmanned Aerial Vehicle (UAV) Remote Sensing. *Agronomy* **2025**, *15*, 434.

<https://doi.org/10.3390/agronomy15020434>

Copyright: © 2025 by the authors. Licensee MDPI, Basel, Switzerland. This article is an open access article distributed under the terms and conditions of the Creative Commons Attribution (CC BY) license (<https://creativecommons.org/licenses/by/4.0/>).

1. Introduction

Crop production is vulnerable to extreme climatic events. Based on global climate change patterns, the modified CERES-Maize model projected the occurrence of extreme precipitation events to increase by 30% by the year 2030 in comparison to 2002, which could lead to potential annual crop production losses amounting to USD 3 billion in the

USA [1]. Frequent excessive rainfall at unfavorable times raises concerns about waterlogged conditions affecting field crops [2].

Flooding emerges as one of the most detrimental abiotic stresses besides drought [3]. From 1951 to 2016, the estimated global average yield losses in soybean, rice, wheat, and maize from flooding were 4, 3, 2, and 1% [4]. A total of 1369 flood events were recorded from 2011 to 2021 in the public global database maintained by G.R. Brakenridge (<http://floodobservatory.colorado.edu>) (accessed on 29 May 2024), out of which, 117 events were recorded in the USA. In addition to creating difficulty in operating field machinery, waterlogged fields also affect nutrient management, especially nitrogen (N). This can be highly problematic, since approximately half of the global population relies on food grown using N-based fertilizers [5]. It contributes significantly (around 41%) to the yield in U.S. maize (*Zea mays* L.) [6]; however, more than 50% of applied N is lost through leaching [7]. N is a mobile nutrient in the soil, available in the nitrate form (NO_3^-), and can easily be lost through processes such as runoff and leaching, especially during heavy rainfall soon after the N application [8,9]. This leads to N deficiency in crops and increased groundwater pollution [9].

Due to its significant contribution to the overall budget of maize crop production, the efficient use of N fertilizer is critical for profitability. Management techniques that decrease N loss in the soil, while simultaneously enhancing N utilization efficiency and crop yield, would be a crucial approach for mitigating the potential adverse impacts of soil waterlogging in the short term [10]. Many farmers in the USA apply the entire amount of N fertilizer in a single dose before the V6 stage, making N fertilizer prone to losses from heavy rainfall events. Due to an increase in climate uncertainties, the arrival of heavy rain soon after N fertilizer applications is becoming a more frequent occurrence, raising concerns for potential N loss, which may negatively impact profitability.

The assessment of the N status involves two main approaches: lab-based analysis and remote sensing-based analysis. While traditional lab analysis ensures accuracy, its extensive, invasive, and point data nature, particularly in dealing with numerous samples and diverse field conditions, limits its practicality. In contrast, remote sensing has proven to be an efficient and non-destructive tool, widely utilized for the rapid estimation of crop N status [11]. Remote sensing techniques use the solar reflective range, which is highly informative in assessing canopy variables such as leaf area index (LAI) and chlorophyll content. This approach facilitates the evaluation of the crop's N status by examining its correlation with chlorophyll content [12]. Utilizing sensors mounted to unmanned aerial vehicles (UAVs), one can estimate vegetation indices (VIs), which are valuable predictors for the levels of chlorophyll and N content in plants [13].

Vegetation indices (VIs) refer to combinations of surface reflectance at two or more wavelengths, strategically designed to accentuate specific properties of vegetation. The normalized difference vegetation index (NDVI) is the most common vegetation index and has a high correlation with plant height [14]. The formula for NDVI is as follows [15]:

$$\text{NDVI} = (\text{rNIR} - \text{rRed}) / (\text{rNIR} + \text{rRed}) \quad (1)$$

where rNIR is the reflectance of the near infrared band (840 nm) and rRed is the reflectance of the red band (668 nm).

As for the leaf nitrogen content, the normalized difference red edge (NDRE) index is more relevant [14] and less susceptible to the saturation problem inherent in the NDVI [16]. The formula for NDRE is similar to that of the NDVI but replaces the red band with a red-edge band, which is more sensitive to changes in the chlorophyll content in plants [17].

Unmanned aerial vehicles, commonly known as drones, are a remotely controlled aircraft that can carry several types of sensors, such as Red-Green-Blue (RGB), multispec-

tral and hyperspectral sensors [18], which allow UAVs to capture aerial images during operation. UAV-based remote sensing systems represent a significant advancement in precision agriculture, as monitoring crops using UAVs provides a simpler, quicker, and more cost-effective way to collect field data compared to older methods [19]. Previous studies have explored aircraft systems for remote monitoring and on-site control. Opportunities exist to investigate the merit of UAV remote sensing technology in assessing mitigation strategies with additional N fertilizer (known as rescue N) to address N loss driven by extreme precipitation events [20].

The objectives of this study were to (1) investigate the effect of excessive moisture conditions on maize yield and economically optimum N rates and (2) evaluate the feasibility of UAV remote sensing for real-time N status monitoring in maize under such abiotic constraints. The overarching aim of the study is to enhance crop production resiliency to extreme climatic events by facilitating informed decision making in agronomic crop nutrient management.

2. Materials and Methods

2.1. Study Sites and Design

This study involved field trials in 2 geographical sites differing in ecoregions and climate types in Louisiana, USA, namely the Doyle Chambers Central Research Station (CRS) in Baton Rouge (Mississippi valley plain ecoregion with subhumid subtropical climate) and the Red River Research Station (RRS) in Bossier city (Red River bottomlands ecoregion with subhumid warm temperate climate) (Figure 1). The research experiments were conducted during the northern hemisphere summer season in 2022 and 2023. The soil type of the experimental fields in these study sites are shown in Table 1. A split-plot design with 4 replications was used with the two water treatments, non-flooded (W1) vs. flooded (W2), as the main plots and different N rates as sub-plots. An Urea Ammonium Nitrate (UAN) blend (20N 4P 4K 2S) was used as the N fertilizer product at the CRS site, whereas Urea Ammonium Nitrate (UAN) (32-0-0) was used as the N fertilizer product at the RRS site. The N treatments consisted of four rates ($0, 45, 179, 224 \text{ kg N ha}^{-1}$) in 2022 and five rates ($0, 45, 135, 224, 269 \text{ kg N ha}^{-1}$ at RRS and $0, 45, 179, 224, 269 \text{ kg N ha}^{-1}$ at CRS) in 2023, applied between V4 (~18–22 days after sowing, DAS) and V5 (~23–27 DAS) stages. The size of individual experimental units was 110 and 38 m^2 for CRS 2022 and 2023, respectively, with the total experimental area of 3519 and 1719 m^2 for CRS 2022 and 2023, respectively. The size of individual experimental units was 68 and 63 m^2 for RRS 2022 and 2023, respectively, with the overall experimental area of 2635 and 2936 m^2 for RRS 2022 and 2023, respectively.

Table 1. Soil type of the study locations at LSU AgCenter Red River Station (RRS) and LSU AgCenter Central Research Station (CRS).

Site Year	Soil Type and Description
RRS, 2022	LaA-Latanier clay, 0 to 1% slopes
RRS, 2023	Fine sandy loam to silt loam, 0 to 1% slopes
CRS, 2022	54.9% CmA-Cancienne silt loam, 0 to 1 percent slopes 45.1% ThA-Thibaut silty clay, 0 to 1 percent slopes
CRS, 2023	27.6% CmA-Cancienne silt loam, 0 to 1% slopes 72.4% ThA-Thibaut silty clay, 0 to 1% slopes

In both study sites, the maize cultivars DKC-70-27 and DKC-65-93 were used in 2022 and 2023, respectively. Maize was planted on 28 March 2022 and 14 April 2023 at the CRS site and on 28 March 2022 and 18 April 2023 at the RRS site, with row planters on beds with furrows

to facilitate water drainage in the field; row spacing was 1.02 m. Excessive water was applied using poly pipes at the RRS location in both years. At CRS, sprinklers were used in 2022, and a 5 cm irrigation hose was used to directly apply water to furrows in 2023. At both sites, excessive water treatment was induced no less than one day after nitrogen application. The downstream ends of the furrows were blocked prior to the initiation of irrigation to effectively flood the W2 treatments. The total estimated excessive water applied was 88 mm within a 5 h period. At the same time as the water provision to the W2 plots, the control plots (W1) also received 36 mm irrigation to bring control plot fields to field capacity. Water inputs and daily mean temperature during the growing season at the study sites are shown in Figure 2.



Figure 1. Maize flooding and N rate study sites. Fields H and C were used for the study trials at LSU AgCenter Red River Research Station (RRS) in 2022 and 2023, respectively. Fields 31 and 33 were used for the study trials at LSU AgCenter Central Research Station (CRS) in 2022 and 2023, respectively. Designation letters and numbers for the fields of interest and the surrounding ones are shown in the station maps.

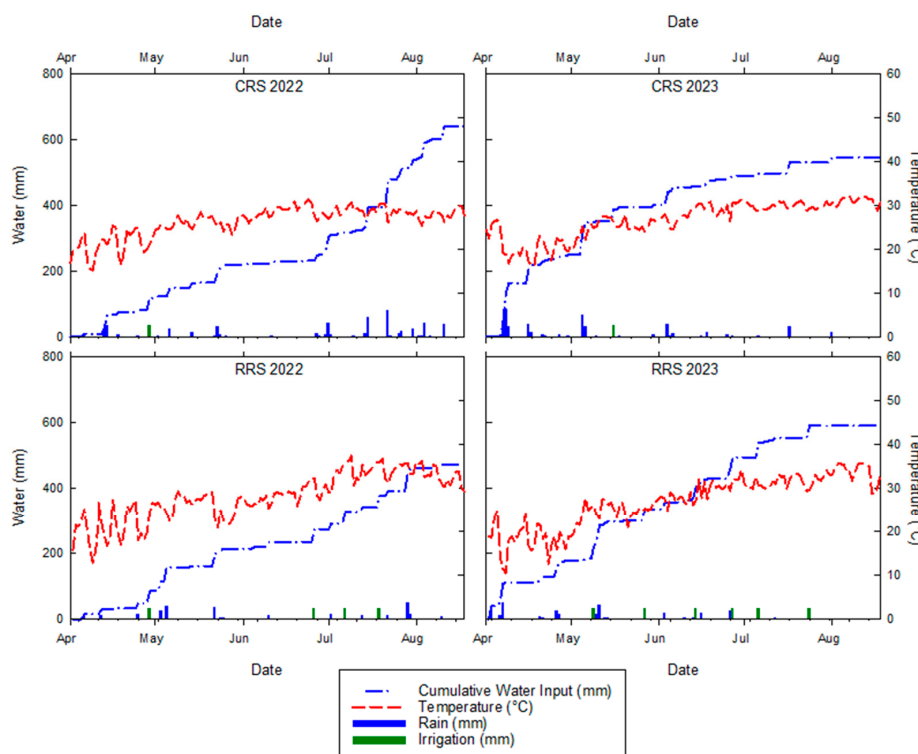


Figure 2. Water input (mm) and mean daily temperature (°C) during the maize growing season at the study sites. CRS: LSU AgCenter Central Research Station. RRS: LSU AgCenter Red River Station.

2.2. Data Collection and Computation of Economically Optimum N Rates (EONR)

During the growing season, UAV flights were carried out in mid-May (V12 to V14), early June (V14 to R1), and late June (R2-R3) using a multicopter UAV (DJI Matrice 300 RTK, Shenzhen, China) aircraft carrying a multispectral sensor (MicaSense Red Edge-MX, Seattle, WA, USA) and supported with a real-time kinematic (RTK) base station (DJI D-RTK2, Shenzhen, China). For each data acquisition, a single flight mission was programmed with DJI Pilot 2 software (accessed on 27 July 2023) to cover the entire experimental area, with the camera capture set to 80% overlaps for both horizontal (side) and vertical (front) directions. The speed of the UAV flight was programmed at 4.1 m s^{-1} , with data capture set to a distance interval. The type of spectral band and center wavelength for this sensor are as follows: Blue (475 nm), Green (560 nm), Red (668 nm), Red Edge (717 nm), and NIR (840 nm). The flights were programmed at 40 m altitude, resulting in 2.88 cm ground sampling distance and scheduled between 9 and 11 a.m. The multispectral data were subjected to camera and sun irradiance radiometric calibration during the flight to mitigate varying sky conditions during data collection missions. The orthomosaic reflectance data were generated using Pix4Dmapper [21], involving computation of key points to find matches between input images and optimization of camera parameters during initial processing (step 1), creation of tie points and three-dimensional texture mesh during point cloud and mesh processing (step 2), and creation of orthomosaic and reflection maps (step 3). During Pix4Dmapper processing step 1, ground control point coordinate data from the four corners of the target fields were provided, with the geographical positional data established using the real-time kinematic (RTK) technique previously described [22]. In the subsequent processing, the Geospatial Data Abstraction Library (GDAL) [23] was used to generate layers composed from individual raster files of the five multispectral bands, with the following order: Red, Green, Blue, Red Edge, and NIR. These remote sensing data were subjected to post-processing steps consisting of raster data compression, pyramiding, and virtual raster creation using GDAL scripts. The remote sensing index, NDRE, was calculated using the raster calculator in QGIS [24]. The mean reprojection error of orthophoto was 0.163 pixels.

The formula for calculating NDRE to estimate N status in maize is as follows [25]:

$$\text{NDRE} = (\text{rNIR} - \text{rRE}) / (\text{rNIR} + \text{rRE}) \quad (2)$$

where rNIR is the reflectance of the near infrared band (840 nm) and rRE is the reflectance of the red edge band (717 nm). The average values of NDVI (Equation (1)) and NDRE were computed using zonal statistics in QGIS for each experimental unit.

Yield data were collected using a plot combine harvester Kincaid 8XP (Kincaid, Haven, KS, USA) equipped with a HarvestMaster GrainGage cereal and small grain yield measurement instrument (Juniper Systems, Logan, UT, USA) from the two middle rows in each experimental unit on 18 August 2022 and 28 August 2023 at the CRS site and on 18 August 2022 and 6 September 2023 at the RRS site. Maize yield data were adjusted based on the actual moisture at harvest and the standard moisture of 15.5%. The spherical function was used to determine yield vs. N rates [26,27], as follows:

$$y = Y_0 + (3Y_a/2\tau) + \theta_3 x^3 \quad (3)$$

$$\tau = 3(Y_a - Y_0)/2\theta_1 \quad (4)$$

where τ is the N rate (represented by x) when the yield (represented by y) reaches the maximum attainable yield, Y_a (Mg ha^{-1}). This spherical function for yield response to

N rate can be reversed using Cardan's solution [28] to solve for the N rate for a given yield target (y):

$$x = 2\tau \cos\left(\left(4\pi + \cos^{-1}(y/Y_a)\right)/3\right) \quad (5)$$

The SciPy artificial intelligence library [29] was used to determine θ_1 and θ_3 parameters in Equations (4) and (5), involving the use of the curve fit function under the subpackage optimizer. The function solves the non-linear spherical parameters by minimizing the sum of the squares of the residuals. The optimization algorithm was written in python programming language in the Jupyter Notebook environment. The economically optimum N rate (EONR) was determined by converting Equation (3) into the net return to N (NRN) Equation involving the price of N fertilizer, P_f (USDkg⁻¹) and maize grain market price, p_g (USDkg⁻¹) and solving x when the first derivative of this Equation equals zero [27]:

$$r_{nf} = p_g(Y_0 + \theta_1 x + \theta_3 x^3) - P_f x \quad (6)$$

$$df(x)/dx = \theta_1 p_g + 3\theta_3 p_g x^2 - P_f = 0 \quad (7)$$

$$EONR = \sqrt{\left(P_f - \theta_1 p_g\right)/(3\theta_3 p_g)} \quad (8)$$

A maize grain price of 0.093 (USDkg⁻¹) and N price of 0.622 (USDkg⁻¹) were used for the computation of EONR in this study based on data from USDA-NASS [30]. Equation (8) for EONR differs from that previously described [27] because in this the study polynomial parameters (θ_1 and θ_3) of the spherical function (Equations (3) and (4)) were directly used to solve EONR. This was feasible, as these parameters were retrieved using the SciPy (version 1.5.2) artificial intelligence optimization algorithm. In contrast, the EONR Equation used in Setiyono et al. [27] relies on indirect estimation of the polynomial parameters based on attainable yield, yield without N supplement, and N rate as the yield approaches attainable yield.

2.3. Statistical Analysis

The two years of data were analyzed in R version 4.3.2 [31] using packages readxl [32], car [33], multcomp [34], ggplot2 [35], and gridExtra [36]. Prior to analyzing the data, the assumptions for ANOVA were checked. The Shapiro–Wilk test was performed to check the normality of residuals, and Levene's test was conducted to check the homogeneity of variance. Multiple two-way fixed effect analysis of variance (ANOVA) was performed for each year, to analyze the treatment means and their variations statistically. The variations among the treatment means were evaluated at a 5% confidence level ($p \leq 0.05$), and a Tukey's Honestly Significant Difference (HSD) test was conducted as a post hoc test to separate treatment means.

3. Results

3.1. N Response Curve and EONR

Almost all field experiments showed an increase in maize yield with increased N fertilization, except for RRS 2023 (Figure 3). The EONR analyses were only feasible for the CRS site due to the lack of plateau segment of the yield response to N at the RRS site in 2022 and the lack of yield response to N in 2023. The fitted spherical functions for CRS 2022 for W1 (control) and W2 (excessive water) treatments were almost identical, with a computed EONR of 157 kg N ha⁻¹ for both treatments and a maximum net return to N at USD 1203 ha⁻¹. In 2023, the analysis suggested a lower maximum attainable yield in excessive water conditions, with the aEONR under the W2 treatment slightly higher at 197 kg N ha⁻¹ as compared to 185 kg N ha⁻¹ in the control treatment, resulting in a

lower maximum net return to N at USD 884 ha^{-1} as compared to USD 1019 ha^{-1} in the control treatment.

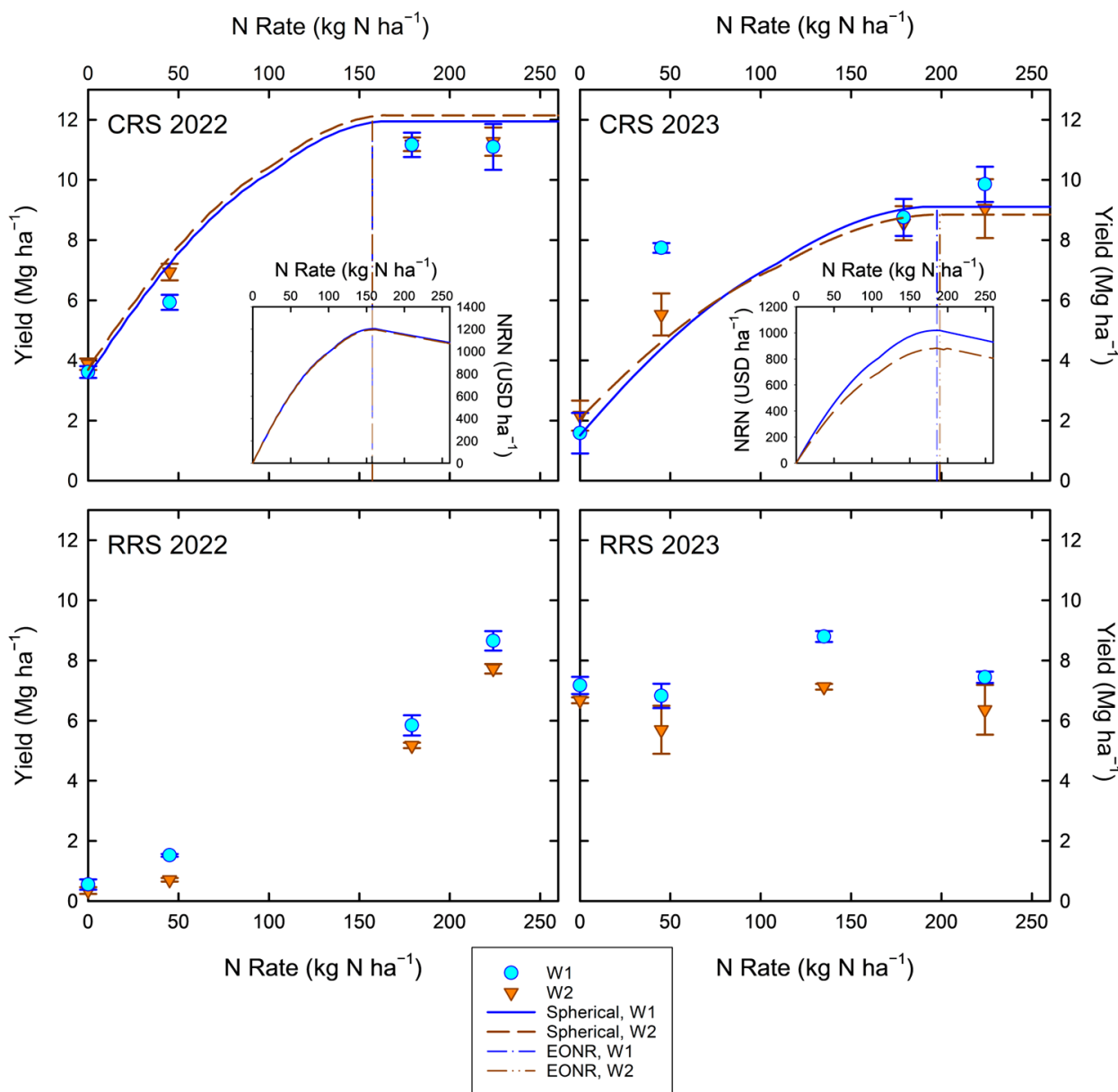


Figure 3. Yield response to N in this study and N response curve as described with spherical function for the CRS site and the corresponding EONR and net return to N, comparing the control (W1) and excessive water conditions (W2). CRS: LSU AgCenter Central Research Station. RRS: LSU AgCenter Red River Research Station. EONR: Economically Optimum N Rate.

3.2. Treatment Effects on Yield

The Shapiro–Wilk normality test for each site year showed that all sites and years had normally distributed residuals, except for RRS 2023. The computed yield skewness and kurtosis for RRS 2023 data of -0.89 and 1.8 , respectively, indicating only slight or moderate non-normality [37], justified the inclusion of these data in ANOVA. Levene's test showed all yield data in this study met the homogeneity of variance assumption. The effects of flooding conditions and N rates on maize yield in each site and year are shown in Tables 2 and 3. The two-way fixed-effect ANOVA on the data showed that in both years, there was a high, significant effect of N rates ($p \leq 0.01$) and flooding ($p \leq 0.0001$) conditions on yield at RRS, whereas only N rates ($p \leq 0.0001$) showed a high, significant effect on yield

at CRS. Yield did not significantly change due to flooding conditions at CRS in both years. In addition, there was no significant effect on yield due to interactions between flooding and N rates in all sites by year.

Table 2. Statistical significance of N rates, flooding treatment, and their interactions with regard to maize yield at Red River Station (RRS) and Central Research Station (CRS) study locations in 2022 and 2023.

Treatments	RRS 2022	RRS 2023	CRS 2022	CRS 2023
N Rates	$<2 \times 10^{-16} *$	0.00196 *	$<2 \times 10^{-16} *$	$7.85 \times 10^{-11} *$
Flooding/No flooding	$7.36 \times 10^{-5} *$	$7.1 \times 10^{-5} *$	0.199	0.157
N rates * Flooding	0.275	0.579	0.605	0.474

* Significant at the 5% probability level by the F test.

Table 3. Maize yield loss from the excessive water treatment in each N treatment at Red River Station (RRS) and Central Research Station (CRS) study sites in 2022 and 2023.

Location	N Rates Kg ha ⁻¹	Yield Loss % 2022	N Rates Kg ha ⁻¹	Yield Loss % 2023
RRS	0	36.2 ns	0	6.9 ns
	45	53.5 ns	45	16.5 ns
	179	11.4 ns	135	19 ns
	224	10.7 *	224	14.6 ns
CRS			269	20.2 ns
	0	−7.2 ns	0	−37 ns
	45	−17 ns	45	28.6 ns
	179	−0.2 ns	179	2.2 ns
	224	−1.6 ns	224	8.2 ns
			269	9.1 ns

* Significant, ns non-significant.

For the post hoc test, a Tukey HSD was chosen to explore the differences in means. Based on the results, at RRS in 2022, increasing the rate of N significantly improved maize yield in non-flooded conditions. In flooded conditions, the yield did not significantly differ between 0 and 45 kg N ha⁻¹. However, beyond 45 kg N ha⁻¹, the yield began to increase significantly with further increases in N rate. In 2023, increasing N rates did not significantly improve the maize yield, confirming the lack of N response shown in Figure 3, but significant loss in yield was seen due to flooding. At CRS, in 2022 and 2023, increasing N improved yield significantly until 179 kg N ha⁻¹, after which yield did not increase significantly upon increasing N rate in both flooded and non-flooded conditions, confirming the plateau nature of yield response as shown in Figure 3.

3.3. Vegetation Indices Response to Treatments

The application of higher fertilizer N rates positively influenced plant health and vigor as reflected in the higher NDRE and NDVI values shown in Figures 4 and 5. Labels in Figures 4 and 5 represent plot code, with the associated water and nitrogen rate treatments listed in Table 4. These figures spatially demarcate plants with lower N content, especially in flooded conditions. In the maps, pixels with color toward a brown hue had low vegetation index (VI) values while those with color toward a green hue had high VI values (Figures 4 and 5). Furthermore, at higher N rates, a reduced spatial variability was observed in the NDRE and NDVI values. Soil test results in the study sites indicated adequate P and K levels; therefore, there was likely a negligible impact of maize growth and yield response to the slight addition of P and K at the CRS site with the N treatments.

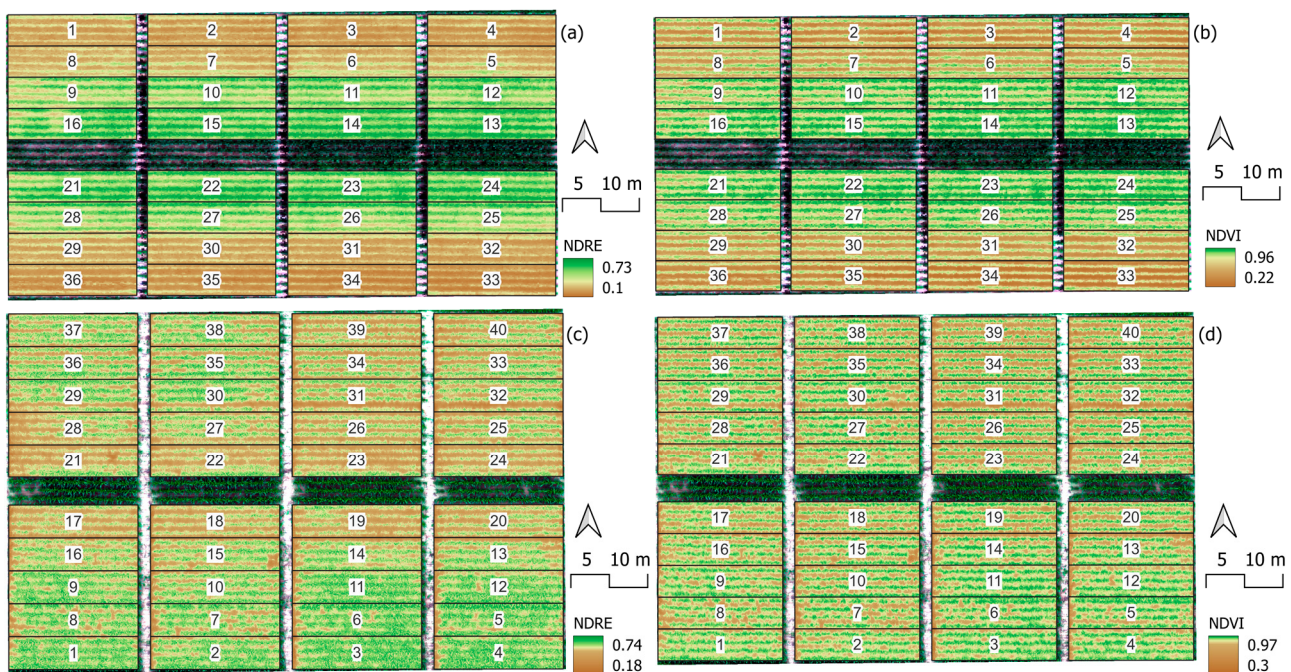


Figure 4. Maps of normalized difference red edge (NDRE) and (a) normalized difference vegetation index (NDVI) (b) sensed on 23 June 2022 for field H LSU AgCenter Red River Research Station (RRS) in Bossier City, LA, USA. The corresponding NDRE and NDVI maps for the sensing date of 12 June 2023 for field C in this site are shown in panels (c) and (d), respectively. The associated water and N rate treatments for the given plot designation in these maps are listed in Table 4.

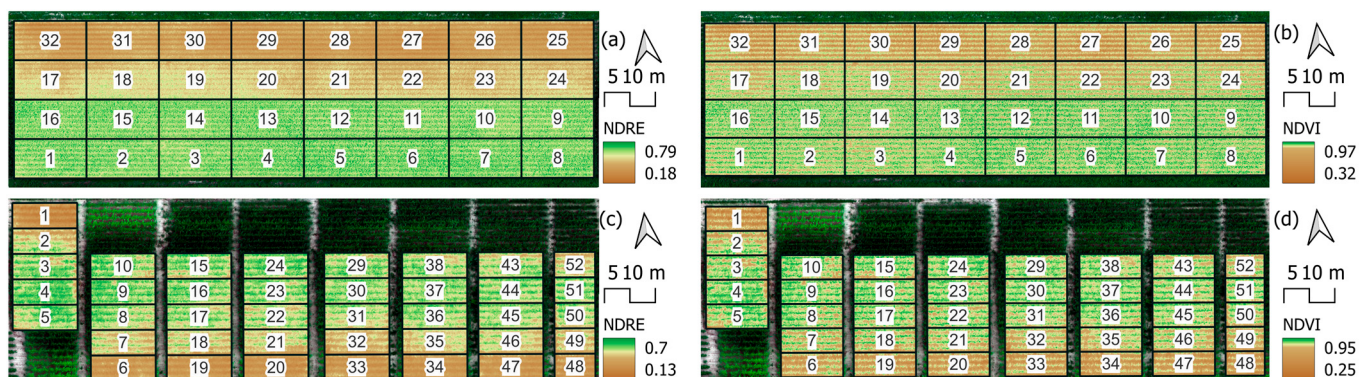


Figure 5. Maps of normalized difference red edge (NDRE) and (a) normalized difference vegetation index (NDVI) (b) sensed on 9 June 2022 for field 31 LSU Central Research Station (CRS), Baton Rouge, LA, USA. The corresponding NDRE and NDVI maps for the sensing data of 8 July 2023 for field 33 in this site are shown in panels (c) and (d), respectively. The associated water and N rate treatments for the given plot designation in these maps are listed in Table 4.

Analysis results between vegetation indices, VIs (NDRE and NDVI), collected at different times during the growing season and maize yield are shown in Figure 6. The VI data collected in mid-May, (V12–V14) or (~50 to ~55–65 DAS), were poorly correlated with maize yield, as was the case for the NDRE data from late June, (R2–R3) or (~80–90 to ~95–110 DAS). The VI data from early June, on the other hand, showed strong correlation with maize yield. The NDRE had a slightly better correlation, with an R^2 of 0.74, as compared to NDVI (R^2 of 0.64). Given this superior performance of NDRE, specifically for the early June data, the subsequent analysis is focused on this vegetation index collected in this time frame (early June, V14–R1, ~55–65 to 65–75 DAS).

Table 4. Plots (as shown in Figures 4 and 5) and the associated water and N rate treatment at Red River Station (RRS) and Central Research Station (CRS) study sites in 2022 and 2023.

Plot No.	Water	N Rate	Plot No.	Water	N Rate
Field H, RRS, 2022			Field H, RRS, 2022		
1, 2, 3, 4	W1	0	33, 34, 35, 36	W2	0
5, 6, 7, 8	W1	45	29, 30, 31, 32	W2	45
9, 10, 11, 12	W1	179	25, 26, 27, 28	W2	179
13, 14, 15, 16	W1	224	21, 22, 23, 24	W2	224
Field C, RRS, 2023			Field C, RRS, 2023		
17, 18, 19, 20	W1	0	21, 22, 23, 24	W2	0
13, 14, 15, 16	W1	45	25, 26, 27, 28	W2	45
9, 10, 11, 12	W1	135	29, 30, 31, 32	W2	135
5, 6, 7, 8	W1	224	33, 34, 35, 36	W2	224
1, 2, 3, 4	W1	269	37, 38, 39, 40	W1	269
Field 31, CRS, 2022			Field 31, CRS, 2022		
29, 30, 31, 32	W1	0	25, 26, 27, 28	W2	0
17, 18, 19, 20	W1	45	21, 22, 23, 24	W2	45
13, 14, 15, 16	W1	179	9, 10, 11, 12	W2	179
1, 2, 3, 4	W1	224	5, 6, 7, 8	W2	224
Field 33, CRS, 2023			Field 33, CRS, 2023		
1, 6, 19, 20	W1	0	33, 34, 47, 48	W2	0
2, 7, 18, 21	W1	45	32, 35, 46, 49	W2	45
5, 8, 17, 22	W1	179	31, 36, 45, 50	W2	179
4, 9, 16, 23	W1	224	30, 37, 44, 51	W2	224
3, 10, 15, 24	W1	269	29, 38, 43, 52	W1	269

W1, Water Control; W2, Excessive Water (Flooded); N Rate, (kg ha^{-1}). RRS: LSU AgCenter Red River Research Station; CRS: LSU AgCenter Central Research Station.

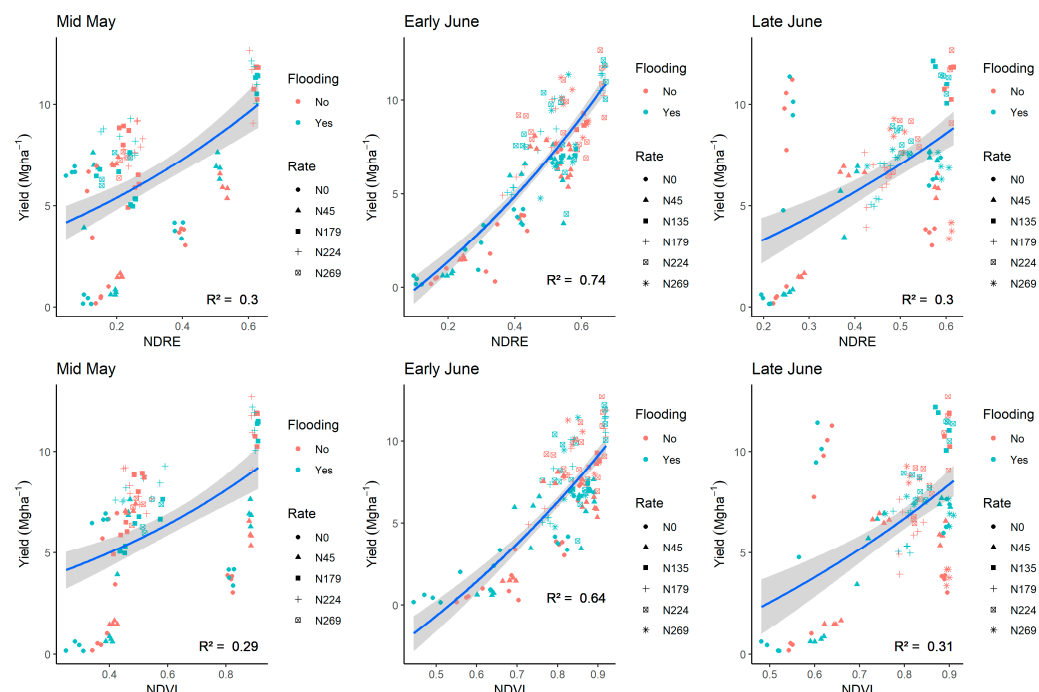


Figure 6. Relationship of vegetation indices (NDRE and NDVI) collected in mid-May (CRS 2022 and 2023, and RRS 2022), early June (CRS 2022 and 2023, and RRS 2022 and 2023), and late June (RRS 2022 and 2023, and CRS 2023) with maize yield. CRS: LSU AgCenter Central Research Station. NDRE: normalized difference red edge. NDVI: normalized difference vegetation index. Blue lines represent fitted regression lines. Grey areas surrounding the blue lines indicate 95% confidence interval for the regression.

The relationship between early June NDRE and N rates in this study is shown in Figure 7. The quadratic functions described the relationship quite well, with R^2 values greater than 0.9. Based on these functions, NDRE values corresponding to the EONR at the CRS site can be derived as follows: For the control treatment at CRS 2022, the estimated NDRE at EONR was 0.671 (99.62% of maximum NDRE), whereas for the excessive water treatment in 2022, the estimated NDRE at EONR was 0.645 (98.32% of maximum NDRE). For the control in 2023, the estimated NDRE at EONR was 0.540 (99.14% of maximum NDRE), whereas the excessive water treatment exhibited an NDRE of 0.507 at EONR (98.38% of maximum NDRE).

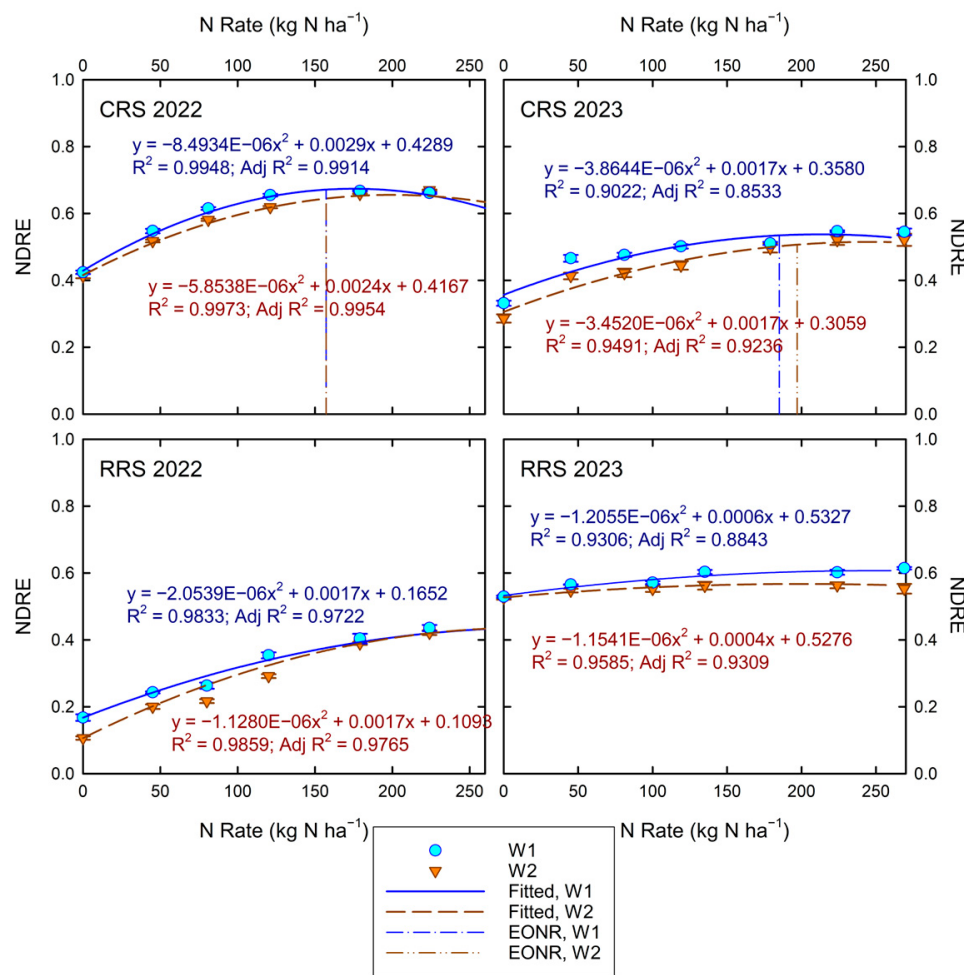


Figure 7. Quadratic (fitted) relationship of early-June NDRE with N rate in this study. For the CRS site, the graphs include the estimated NDRE values at the computed EONR, comparing the control and excessive water conditions. Additional data points between N rates of 70 to 130 were based on reconstructed data using the yield VI relationship in Figure 6 and yield response to N rate in Figure 3.

4. Discussion

The CRS 2022 showed higher yield in excessive moisture conditions due to a drought spell during mid-May to mid-June (Figure 2). The weather data also showed higher daily average temperature during the growing season in 2022 at CRS as compared to 2023. The excessive water applied early in the season resulted in higher residual moisture, which mitigated a portion of the drought effects, which were more important than N losses. At the RRS site in 2023, maize yield did not respond to increasing N rates, and this is suspected to be due to the high amount of residual N from the previous crop (severely drought affected maize) (Figure 2). Additionally, excessive water negatively impacted maize yield at RRS but not necessarily at CRS, highlighting the variability in environmental conditions and

soil types between the two locations, which affected N losses through leaching, runoff, volatilization, and NO_x emissions. Further climatic differences between the two locations include slightly greater total solar radiation, warmer temperatures during the off-season, and wetter climate based on the number of rain days and long-term mean monthly rain at CRS as compared to RRS. Such climatic differences can cause differences in terms of soil microbial activity in these locations, which may alter the resiliency of the soil system to loss of N from excessive moisture.

A novel component included in this study, the characterization of the N response curve with the spherical function [27], with parameters optimized using SciPy artificial intelligence algorithm, allows deeper understanding of the excessive water conditions in terms of the effect on EONR and net return to N. For example, at the CRS site in 2023, the excessive water condition caused EONR to be about 12 kg N ha⁻¹ higher, while the attainable yield was reduced by 8%, resulting in a 13% reduction in net return to N. Given the typical N rates, the experiment attempted to solve for the optimum N rate, which is of interest for practical applications. The straightforward statistical analysis of each N rate treatment lacks relevancy to the real-world situation and therefore should not be the ultimate source of information for inferring the agronomic response of maize N fertility to excessive water post-fertilizer application. The number of N rates increased from four to five between 2022 and 2023, to improve the response curve analysis. Nonetheless, the use of four rates to derive the N response curve has been done before [38] with success.

The NDRE and NDVI maps shown in Figures 4 and 5 clearly indicate the areas where maize plants have a lower N content based on the analysis. This fact can help growers decide whether supplemental N is needed or not after an adverse condition such as excessive rain. Lower spatial variability was noticed at higher N rates, suggesting that an adequate provision of N to the crop creates a more uniform growth across space, as the crop reaches a saturation point beyond which additional N does not result in significant improvements in plant health.

The high correlation between maize yield and vegetation indexes at the pre-silking stage in this study (Figure 6), especially NDRE, is reasonable considering the very active growth around this stage, with most of the supplemental N taken up by the plants supporting higher chlorophyll content, photosynthetic rate, biomass production, and canopy coverage [38]. This also explains why N rates and NDRE are well correlated (Figure 6). This finding aligns with other studies reporting a stronger association of NDRE with N rates as compared to NDVI around 61 days after emergence [14,39] which corresponds to the pre-silking stage in our study. Future investigations involving hyperspectral sensors (visible-NIR-SWIR) can further elucidate the detailed mechanism of N dynamics in maize under N-limiting conditions. Nonetheless, separate complementary analyses from the same study provided confirmation that NDRE derived from the multispectral sensor used in this study indeed captured the detailed phenomena of leaf chlorosis induced by N-deficient conditions rather than simply sensing the reduction in canopy cover, as the growth of maize leaves became restricted under N-limiting conditions [22]. The effect of genotype is outside the scope of the present study. Future investigation can be directed toward understanding the possible different response of different maize varieties to N rates and waterlogging.

Using the spherical functions, NDRE at EONR can be derived from the results (Figure 7), revealing an interesting trend. First, the NDRE at EONR under control conditions is roughly at 99% of the maximum NDRE. Such notation justifies the use of N-rich strip and NDRE-based fertilizer N rate recommendations [40]. Under the excessive water after fertilizer application, this study reveals that the NDRE percentage value (percent of the maximum value) was reduced to 98% in 2022 and 2023. Such a phenomena of reduced NDRE values at EONR as a fraction of

the maximum attainable NDRE warrants the importance of such abiotic stress to be considered in the algorithm for deriving N rate recommendations based on the N-rich strip concept.

5. Conclusions

This study suggests a site-specific difference in maize yield response to excessive moisture conditions, with maize yield loss being significant at the RRS but not the CRS site. Further analysis of the optimum N rate captures a reduction of net return, as a higher N rate was required to achieve optimum yield in the case of an excessive moisture environment. The work presented here demonstrates the promising use of UAV remote sensing in characterizing N status under such abiotic stress. Sensing at around V12 (~50 DAS) to R1 (~65–75 DAS) maize phenological stage can be used to evaluate the status of the plants in terms of the level of “greenness” needed to reach optimum N rates. This study reveals a slight reduction of the fraction of NDRE at the optimum N rate to maximum NDRE under the excessive water conditions, highlighting the need for addressing such abiotic stress circumstances when arriving at N rate recommendations based on the N-rich strip.

Author Contributions: Conceptualization, B.A. and T.S.; methodology, B.A., T.G., F.R., R.A., D.D. and T.S.; software, B.A., T.G. and T.S.; validation, B.A. and T.S.; formal analysis, B.A., T.G. and T.S.; investigation, B.A., F.R., G.B. and T.S.; resources, T.S., S.D. and B.T.; data curation, B.A., T.S., S.D., F.R., R.A., D.D. and G.B.; writing—original draft preparation, B.A., R.A., D.D. and T.S.; writing—review and editing, B.A., T.S., S.D., T.G. and B.T.; visualization, B.A.; supervision, T.S.; project administration, T.S.; funding acquisition, T.S., S.D. and B.T. All authors have read and agreed to the published version of the manuscript.

Funding: This research was funded by Louisiana Soybean and Grains Research and Promotion Board, grant number GR-00011336.

Data Availability Statement: The original contributions presented in the study are included in the article. Further inquiries can be directed to the corresponding author.

Acknowledgments: The authors acknowledge Chris Roider, Peters Egbedi, Marcelo Rodrigues Barbosa Júnior, Rajesh Neupane, Aakriti Poudel, Ritik Pokharel, and Sandra Stevenson in supporting the research study and preparations of this manuscript.

Conflicts of Interest: The authors declare that they have no known competing financial interests or personal relationships that could have appeared to influence the work reported in this paper.

References

- Rosenzweig, C.; Tubiello, F.N.; Goldberg, R.; Mills, E.; Bloomfield, J. Increased Crop Damage in the US from Excess Precipitation under Climate Change. *Glob. Environ. Change* **2002**, *12*, 197–202. [[CrossRef](#)]
- Kunkel, K.E. North American Trends in Extreme Precipitation. *Nat. Hazards* **2003**, *29*, 291–305. [[CrossRef](#)]
- Bailey-Serres, J.; Lee, S.C.; Brinton, E. Waterproofing Crops: Effective Flooding Survival Strategies. *Plant Physiol.* **2012**, *160*, 1698–1709. [[CrossRef](#)] [[PubMed](#)]
- Kim, W.; Iizumi, T.; Hosokawa, N.; Tanoue, M.; Hirabayashi, Y. Flood Impacts on Global Crop Production: Advances and Limitations. *Environ. Res. Lett.* **2023**, *18*, 054007. [[CrossRef](#)]
- Erisman, J.W.; Sutton, M.A.; Galloway, J.; Klimont, Z.; Winiwarter, W. How a Century of Ammonia Synthesis Changed the World. *Nat. Geosci.* **2008**, *1*, 636–639. [[CrossRef](#)]
- Stewart, W.M.; Dibb, D.W.; Johnston, A.E.; Smyth, T.J. The Contribution of Commercial Fertilizer Nutrients to Food Production. *Agron. J.* **2005**, *97*, 1–6. [[CrossRef](#)]
- Deutsch, C.; Sarmiento, J.L.; Sigman, D.M.; Gruber, N.; Dunne, J.P. Spatial Coupling of Nitrogen Inputs and Losses in the Ocean. *Nature* **2007**, *445*, 163–167. [[CrossRef](#)] [[PubMed](#)]
- Ortez, O.; LaBarge, G.; Lindsey, A.; Novais, W. Managing Corn and Nitrogen with Water Excess Conditions. *Crop Obs. Recomm. Netw. Newslet.* **2022**, *19*.
- Kaur, G.; Singh, G.; Motavalli, P.P.; Nelson, K.A.; Orlowski, J.M.; Golden, B.R. Impacts and Management Strategies for Crop Production in Waterlogged or Flooded Soils: A Review. *Agron. J.* **2020**, *112*, 1475–1501. [[CrossRef](#)]

10. Kaur, G.; Zurweller, B.A.; Nelson, K.A.; Motavalli, P.P.; Dudenhoeffer, C.J. Soil Waterlogging and Nitrogen Fertilizer Management Effects on Corn and Soybean Yields. *Agron. J.* **2017**, *109*, 97–106. [CrossRef]
11. Lu, N.; Wang, W.; Zhang, Q.; Li, D.; Yao, X.; Tian, Y.; Zhu, Y.; Cao, W.; Baret, F.; Liu, S.; et al. Estimation of Nitrogen Nutrition Status in Winter Wheat from Unmanned Aerial Vehicle Based Multi-Angular Multispectral Imagery. *Front. Plant Sci.* **2019**, *10*, 1601. [CrossRef] [PubMed]
12. Jaberí-Aghdam, M.; Momayyezi, M.R.; Bagheri, N.; Azizi, P.; Nasri, M. Nitrogen Assessment by Remote Sensing and Multispectral Imagery in Maize (*Zea mays* L.). *J. Crop Sci. Biotechnol.* **2023**, *27*, 31–41. [CrossRef]
13. Clevers, J.G.P.W.; Gitelson, A.A. Remote Estimation of Crop and Grass Chlorophyll and Nitrogen Content Using Red-Edge Bands on Sentinel-2 and -3. *Int. J. Appl. Earth Obs. Geoinf.* **2013**, *23*, 344–351. [CrossRef]
14. Flores, M.D.S.; Paschoalete, W.M.; Baio, F.H.R.; Campos, C.N.S.; Pantaleão, A.d.A.; Teodoro, L.P.R.; da Silva Júnior, C.A.; Teodoro, P.E. Relationship between Vegetation Indices and Agronomic Performance of Maize Varieties under Different Nitrogen Rates. *Biosci. J.* **2020**, *36*, 1638–1644. [CrossRef]
15. Rouse, J.; Haas, R.H.; Schell, J.A.; Deering, D. Monitoring Vegetation Systems in the Great Plains with ERTS. In *Third Earth Resources Technology Satellite-1 Symposium-Volume I: Technical Presentations*. NASA SP-351; Freden, S.C., Mercanti, E.P., Becker, M.A., Eds.; NASA: Washington, DC, USA, 1973; pp. 307–317.
16. Rehman, T.H.; Lundy, M.E.; Linquist, B.A. Comparative Sensitivity of Vegetation Indices Measured via Proximal and Aerial Sensors for Assessing N Status and Predicting Grain Yield in Rice Cropping Systems. *Remote Sens.* **2022**, *14*, 2770. [CrossRef]
17. Croft, H.; Chen, J.M. 3.09—Leaf Pigment Content. In *Comprehensive Remote Sensing*; Liang, S., Ed.; Elsevier: Oxford, UK, 2018; pp. 117–142. [CrossRef]
18. Radoglou-Grammatikis, P.; Sarigiannidis, P.; Lagkas, T.; Moscholios, I. A Compilation of UAV Applications for Precision Agriculture. *Comput. Netw.* **2020**, *172*, 107148. [CrossRef]
19. Tsouros, D.C.; Bibi, S.; Sarigiannidis, P.G. A Review on UAV-Based Applications for Precision Agriculture. *Inf. Switz.* **2019**, *10*, 349. [CrossRef]
20. Nelson, K.A.; Scharf, P.C.; Stevens, W.E.; Burdick, B.A. Rescue Nitrogen Applications for Corn. *Soil Sci. Soc. Am. J.* **2011**, *75*, 143–151. [CrossRef]
21. PIX4Dmapper, Version 4.7.5. The Leading Photogrammetry Software for Professional Drone Mapping. Pix4D. Available online: <https://www.pix4d.com/product/pix4dmapper-photogrammetry-software/> (accessed on 24 April 2022).
22. Setiyono, T. Precise Positioning in Nitrogen Fertility Sensing in Maize (*Zea mays* L.). *Sensors* **2024**, *24*, 5322. [CrossRef]
23. Geospatial Data Abstraction Library (GDAL)/OGR Simple Features Library (OGR) Contributors. GDAL/OGR Geospatial Data Abstraction Software Library. Open-Source Geospatial Foundation. Available online: <https://zenodo.org/records/12545688> (accessed on 15 September 2023).
24. Quantum Geographic Information System (QGIS) Development Team. QGIS Geographic Information System. Version 3.28.1. Open-Source Geospatial Foundation. Available online: <http://qgis.org> (accessed on 15 September 2023).
25. Barnes, E.M.; Clarke, T.R.; Richards, S.E.; Colaizzi, P.D.; Haberland, J.; Kostrzewski, M.; Waller, P.; Choi, C.; Riley, E.; Thompson, T.; et al. Coincident Detection of Crop Water Stress, Nitrogen Status and Canopy Density Using Ground Based Multispectral Data. In Proceedings of the 5th International Conference on Precision Agriculture, Bloomington, MN, USA, 16–19 July 2000; Robert, P.C., Rust, R.H., Larson, W.E., Eds.; ASA-CSSA-SSSA: Madison, WI, USA, 2000; pp. 1–15.
26. Dobermann, A.; Wortmann, C.S.; Ferguson, R.B.; Hergert, G.W.; Shapiro, C.A.; Tarkalson, D.D.; Walters, D.T. Nitrogen Response and Economics for Irrigated Corn in Nebraska. *Agron. J.* **2011**, *103*, 67–75. [CrossRef]
27. Setiyono, T.D.; Yang, H.; Walters, D.T.; Dobermann, A.; Ferguson, R.B.; Roberts, D.F.; Lyon, D.J.; Clay, D.E.; Cassman, K.G. Maize-N: A Decision Tool for Nitrogen Management in Maize. *Agron. J.* **2011**, *103*, 1276–1283. [CrossRef]
28. Nickalls, R.W.D. A New Approach to Solving the Cubic: Cardan’s Solution Revealed. *Math. Gaz.* **1993**, *77*, 354–359. [CrossRef]
29. Virtanen, P.; Gommers, R.; Oliphant, T.E.; Haberland, M.; Reddy, T.; Cournapeau, D.; Burovski, E.; Peterson, P.; Weckesser, W.; Bright, J.; et al. SciPy 1.0: Fundamental Algorithms for Scientific Computing in Python. *Nat. Methods* **2020**, *17*, 261–272. [CrossRef] [PubMed]
30. United State Department of Agriculture (USDA). USDA-NASS NASS-Quick Stats. National Agricultural Statistics Service (NASS). Available online: <https://www.nass.usda.gov/services/agdatacommons> (accessed on 20 September 2024).
31. R Core Team. *R: A Language and Environment for Statistical Computing*; R Foundation for Statistical Computing: Vienna, Austria, 2013. Available online: <https://www.r-project.org> (accessed on 15 September 2023).
32. Wickham, H.; Bryan, J. Readxl: Read Excel Files. Available online: <https://readxl.tidyverse.org/> (accessed on 15 September 2023).
33. Fox, J.; Weisberg, S. *An R Companion to Applied Regression*, 3rd ed.; SAGE Publications, Inc.: Thousand Oaks, CA, USA, 2019.
34. Hothorn, T.; Bretz, F.; Westfall, P. Simultaneous Inference in General Parametric Models. *Biom. J.* **2008**, *50*, 346–363. [CrossRef]
35. Wickham, H.; Chang, W.; Henry, L.; Pedersen, T.L.; Takahashi, K.; Claus, W.; Yutani, H.; Dunnnington, D.; van den Brand, T. ggplot2. Available online: <https://ggplot2.tidyverse.org/> (accessed on 15 September 2023).

36. Auguie, B.; Antonov, A. gridExtra: Miscellaneous Functions for “Grid” Graphics. Available online: <https://rdrr.io/cran/gridExtra/> (accessed on 15 September 2023).
37. Lei, M.; Lomax, R.G. The Effect of Varying Degrees of Nonnormality in Structural Equation Modeling. *Struct. Equ. Model.* **2005**, *12*, 1–27. [CrossRef]
38. Vanotti, M.B.; Bundy, L.G. An Alternative Rationale for Corn Nitrogen Fertilizer Recommendations. *J. Prod. Agric.* **1994**, *7*, 243–249. [CrossRef]
39. Jang, C.; Namoi, N.; Wolske, E.; Wasonga, D.; Behnke, G.; Bowman, N.D.; Lee, D.K. Integrating Plant Morphological Traits with Remote-Sensed Multispectral Imageries for Accurate Corn Grain Yield Prediction. *PLoS ONE* **2024**, *19*, e0297027. [CrossRef] [PubMed]
40. Holland, K.H.; Schepers, J.S. Derivation of a Variable Rate Nitrogen Application Model for In-Season Fertilization of Corn. *Agron. J.* **2010**, *102*, 1415–1424. [CrossRef]

Disclaimer/Publisher’s Note: The statements, opinions and data contained in all publications are solely those of the individual author(s) and contributor(s) and not of MDPI and/or the editor(s). MDPI and/or the editor(s) disclaim responsibility for any injury to people or property resulting from any ideas, methods, instructions or products referred to in the content.